

# Automatic horizon tracking algorithm with curvature constraint

Jiji Zhou<sup>1</sup>, Huiqun Xu<sup>\*2</sup>, Ping Yang<sup>3</sup>, Mengqiong Yang<sup>4</sup>

<sup>(1)</sup> School of Geophysics and petroleum resources, Yangtze University, Wuhan 430100, Hubei Province, China

<sup>(2)</sup> School of Geophysics and petroleum resources, Yangtze University, Wuhan 430100, Hubei Province, China

<sup>(3)</sup> BGP, CNPC, Zhuozhou 072751, China

<sup>(4)</sup> School of Geophysics and petroleum resources, Yangtze University, Wuhan 430100, Hubei Province, China

Article history: received August 24, 2022; accepted January 9, 2023

## Abstract

Seismic horizon tracing is a key step in seismic data interpretation. At present, it mainly relies on manual interpretation to mark the layers within the region. The deficiency of manual interpretation lies in its low precision and efficiency, and it relies heavily on the experience of the interpreter. Aiming at the above problems, the author proposes an automatic horizon tracking algorithm with curvature constraint. The algorithm firstly determines the initial seed points of horizon tracking based on logging data, and then generates all seed points by tracing the direction of crossline. According to the seed point, track the horizon by the direction of the inline. The curvature of each horizon point is calculated in the direction of the crossline according to the tracked results. For the layer point that do not meet the ruling curvature threshold, they are traced again in the direction of the crossline, and finally the corrected tracking results are obtained. Through the test of actual data, this method has achieved good results.

Keywords: Seismic exploration; Seismic horizon tracing; Curvature; Seed point; Peak tracking

---

## 1. Introduction

Seismic exploration is a widely used method in geophysical exploration. Artificial earthquakes are created by firing cannons at the epicenter, which further excites seismic waves. By processing and interpreting the reflected signals received, the geological structures deep underground can be obtained. The horizons in seismic data can also reflect the formation of underground rock formations, which plays a fundamental role in predicting and excavating underground energy and mineral resources [Luo, 2014].

There are many methods to realize automatic horizon tracking. It can be roughly divided into four categories (1) horizon tracking method based on artificial neural network [Yuan et al., 2020; Yu et al 2021], Alberts et. al. [1999] proposed an automatic horizon tracking solution based on artificial neural network in 1999, which is a widely used method at present. Bas Peter [Peter et al. 2019] developed a loss function in 2019, which can be used to conduct nonlinear regression training for UNET network and achieve better results with less data. (2) Image-based horizon tracking method [Liu et al., 2017; Cheng et al., 2021]. The seismic profile is treated as a sequence of 2D images.

Li et al. [2007] proposed a method for edge detection of seismic profile images using Canny operator in 2007, which has advantages of tracking speed and low cost. Disadvantage of the method is that the result is poor when it comes to areas with no obvious stratigraphic features. Combining neural network and image classification technology, Yang et al. [2020] proposed using CNN deep convolutional neural network to realize simultaneous automatic multi-layer tracking in 2020, and manually marked the horizon on the picture to train the neural network to learn the characteristics of seismic data and then predict the horizon. (3) Horizon tracing method based on seismic attributes. Labrunye et al. [2015] and Forte et al. [2016] used seismic phase attributes to track horizons in 2015-2016. (4) Horizon tracing method based on seismic coherence. This method can automatically track the in-phase axis based on the similar amplitude of adjacent channels in the same horizon. Li [2005] used the ordinary Kriging method to interpolate data volumes in 2015. In this method, some layer points are selected manually as constraint points, and then the complete layer is obtained by interpolation.

However, when encountering a region with a low signal-to-noise ratio in the region, the above method can't solve it well. Therefore, on this basis, the author proposes a horizon tracking algorithm under the curvature constraint based on the waveform coherence principle. The method firstly determines the initial seed point according to logging curve or manual annotation, and then determines a search time window, calculates the point with the largest amplitude in the search time window and takes it as the next seed point. The seed points are iterated in the 3D seismic data volume until the whole 3D data volume is tracked. The tracking result are corrected in the direction of the crossline. By calculating the curvature of each layer points, for the deviated layer points, the track and correction are carried out in the direction of the crossline, and the final result under the curvature constraint is obtained. The effectiveness of the method is proved by the test of 3D seismic data volume of 110\*142\*401.

## 2. Algorithm Implementation

Relevant implementation strategies are formulated, and the specific implementation steps are shown in Figure 1 and subsequently described.

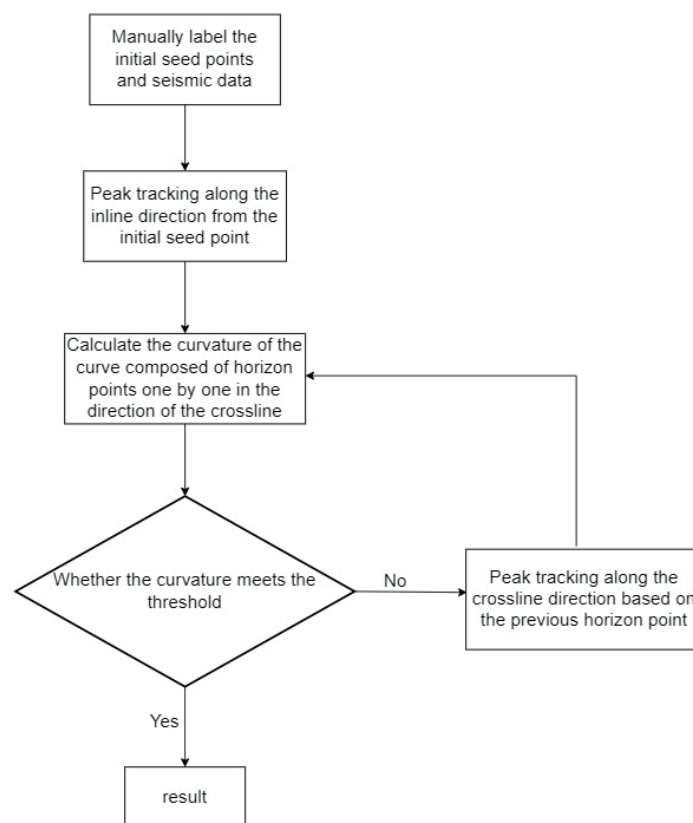


Figure 1. Overall flow chart.

## 2.1 Initial seed point and its selection

A seed point is a known horizon point in a 3D seismic data volume, generally determined from well logging data. Figure 2 is a schematic diagram of the distribution of seed points in the formation. The more seed points the tracking results are more accurate, but in actual production, the number of seed points cannot be infinite because of the limitation of the number of wells. The author chooses to take three initial seed points on each horizon, and the initial seed points track each other to generate the next seed point.

For non-fault locations, the author chooses a profile in the middle of the 3D seismic data volume, and evenly takes three traces on this section, then manually marks the initial seed points of horizons on these three traces (Figure 3). The three initial seed points are traced to the first profile and the last profile to complete the generation of all seed points.

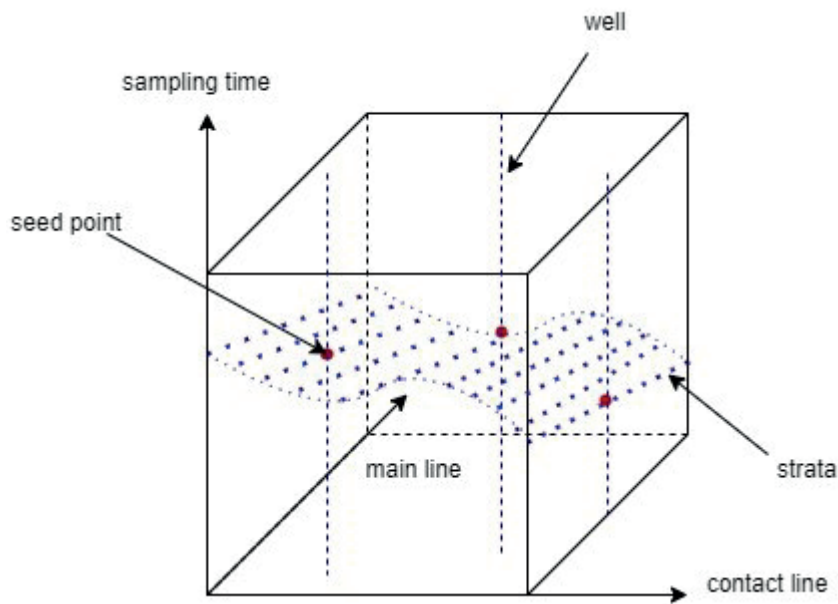


Figure 2. Schematic diagram of the seed point in the formation.

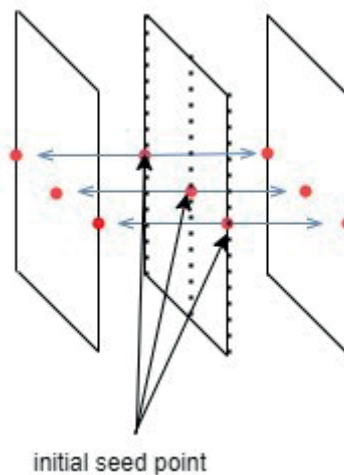


Figure 3. Schematic diagram of seed point generation.

## 2.2 Horizon Tracking

According to the obtained seed points, for each profile, take the first profile as an example. Track from the first seed point to the seed point in the middle of the profile, and track horizon point in the trace one by one (Fig. 4). then from the seed point in the middle of the profile to the seed point of the last profile. As shown in Figure 5. After the tracking is completed, the curvature of each horizon point is calculated on the crossline.

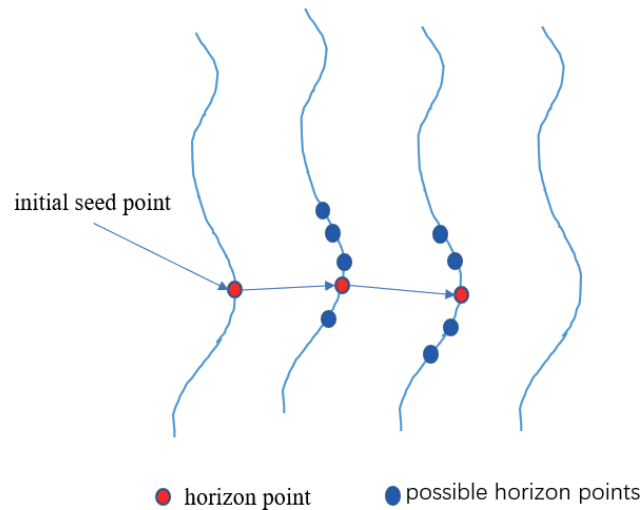


Figure 4. Peak horizon point tracking.

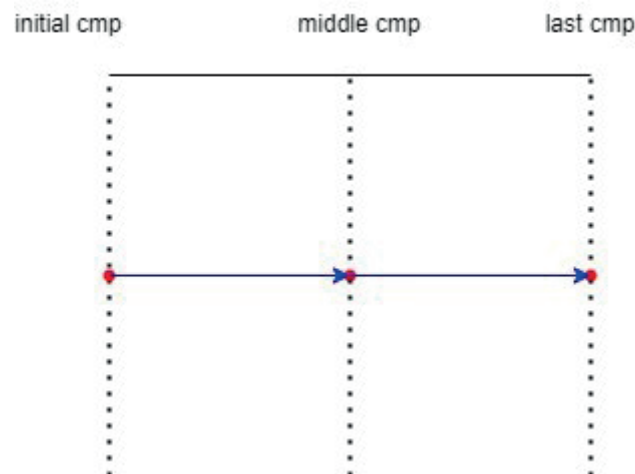


Figure 5. Schematic diagram of tracing on the cross section.

## 2.3 Curvature and horizon line with curvature description

The curvature of seismic horizon line has its unique physical meaning in revealing anticlines and synclines. The curvature of the two-dimensional horizon line can be calculated according to the sampling time, track number or line number in the horizon point coordinates. Figure 6 is an interpretation of the curvature of the horizon line.

For areas with large strata fluctuations, the absolute value of the curvature is larger, and when the stratum is relatively flat, the absolute value of the curvature is smaller. The positive or negative curvature value determines whether the formation undulates up or down, and when a fault is encountered, the curvature becomes infinite. The

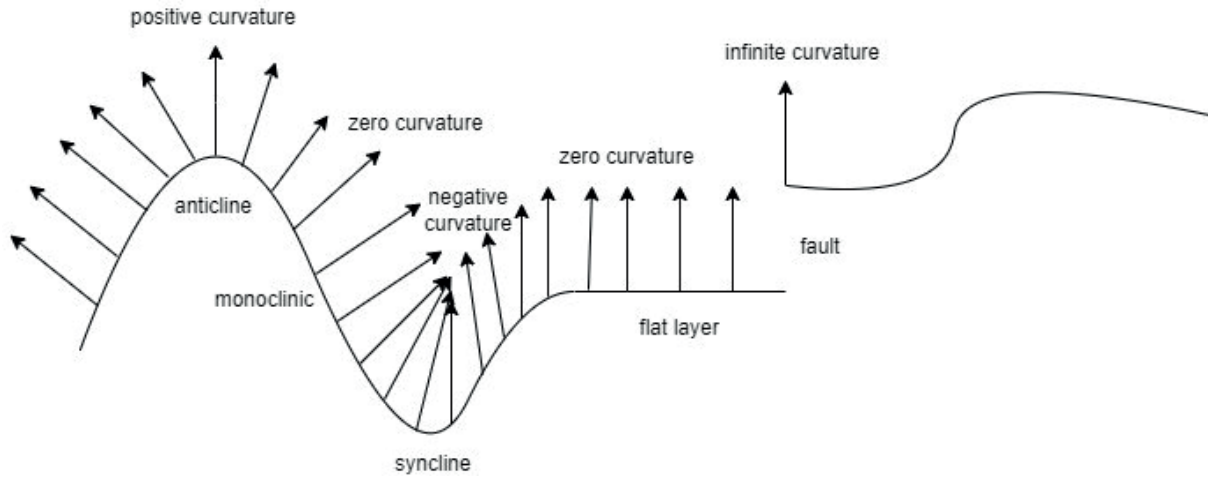
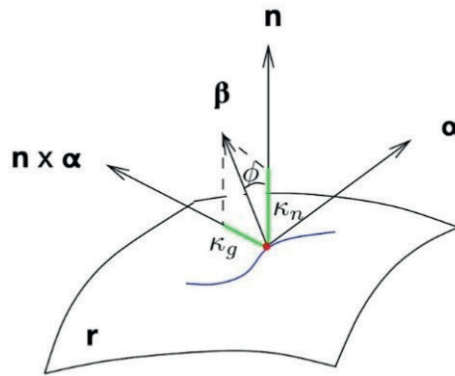


Figure 6. Curvature description of horizon lines.



$\alpha$  is the tangent vector of the curve,  $\beta$  is the normal vector of the curve,  $n$  is the normal vector of the surface

Figure 7. Schematic diagram of surface curvature.

curvature of the horizon can well reflect the structural trend of the underground horizon, and it is an important indicator to measure whether the horizon automatic tracking is correct.

The maximum curvature and geodesic curvature evolved from the normal curvature also have their physical significance in geological structures. Roberts [2001] gave the calculation formula and discussed its application in tectonic interpretation in 2001; Hakami et al. [2004] and Al-Dossary et al. [2006] extended it to formation curvature, and make the application of multi-scale (fractional wave number) analysis to it which makes the interpretation of seismic attributes derive a new field, and has been widely used.

The advanced mathematics defines the curvature of a curve as: the curvature is the rotation rate of the tangent direction angle to the arc length for a certain point on the curve, indicating the degree to which the curve deviates from the straight line in Figure 8.

Since the horizon points are discrete points, here the author takes the curvature of the quadratic curve fitted by every three horizon points as our estimated curvature, and then takes the curvature at the middle horizon point as the curvature of the three horizon points. For a parametric equation of a curve consisting of three points, the curvature at a point can be expressed as a differential [Department of Mathematics, Tongji University, 1996].

$$k = \frac{x''y' - x'y''}{((x')^2 + (y')^2)^{3/2}} \quad (1)$$

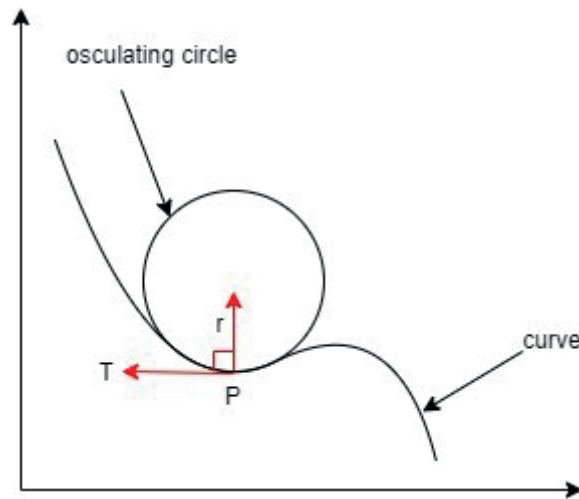


Figure 8. Mathematical definition of curvature.

## 2.4 Layer curvature calculation and result correction

Three horizon points can determine an outer circle, when the next two horizon points approach the middle point, the outer circle is called the osculating circle. In Figure 9, the curvature of the close circle can be calculated by using the formula shown in (1), which is called the curvature of the curve formed by the three horizon points. Curvature is calculated for each group of three result horizon points until all horizon points are calculated.

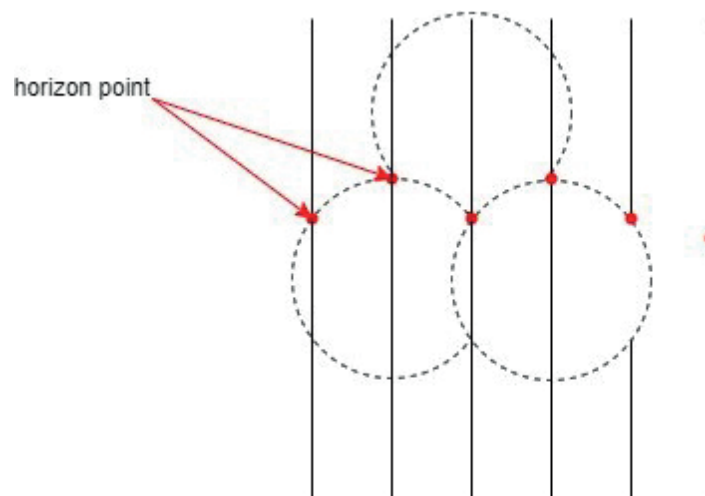
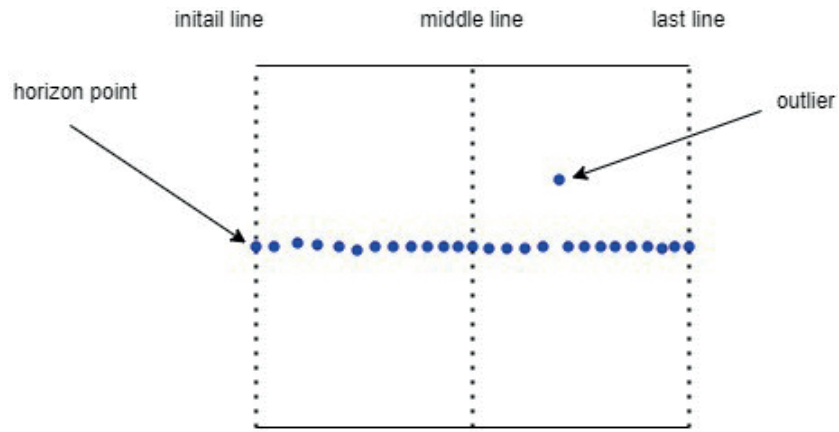


Figure 9. Curvature calculation.

Through the analysis of abnormal areas in the tracking results of actual data as shown in Figure 11, the schematic diagram of curvature distribution as shown in Figure 13 was obtained. The abnormal area of curvature is shown in the circle in the figure. When the curvature exceeds 2 or is between 0 and 0.2, it can be judged as the abnormal area of horizon tracking.

For the extracted horizon points with abnormal curvature (as shown in Figure 10), we take the time of the previous horizon as the benchmark in the direction of the crossline, then continue to track the wave peak value again in the next set-time window, and replace the newly tracked horizon point to original horizon point, finally complete the correction of all horizon. Then we obtain the final tracking result by correcting the abnormal curvature area as is shown in Figure 12.

## Automatic horizon tracking algorithm with curvature constraint



**Figure 10.** Schematic diagram of the direction correction of the crossline.

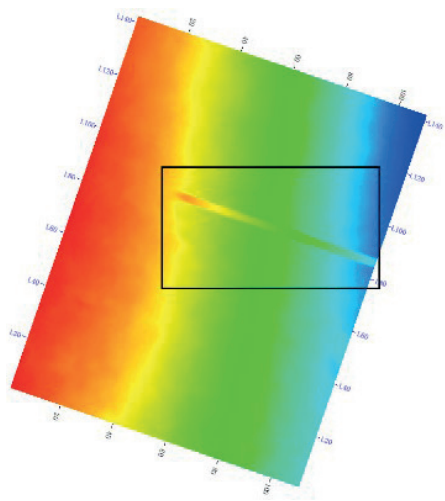


**Figure 11.** Horizon before the correction.

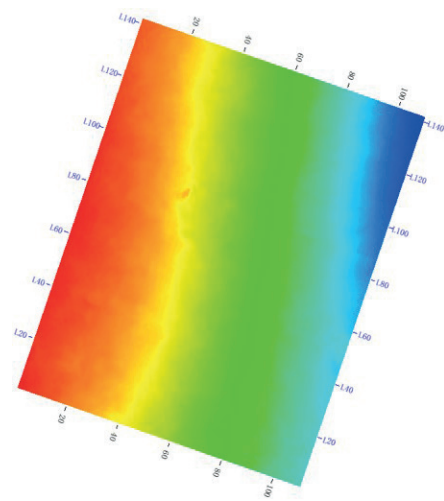


**Figure 12.** Horizon after the correction.

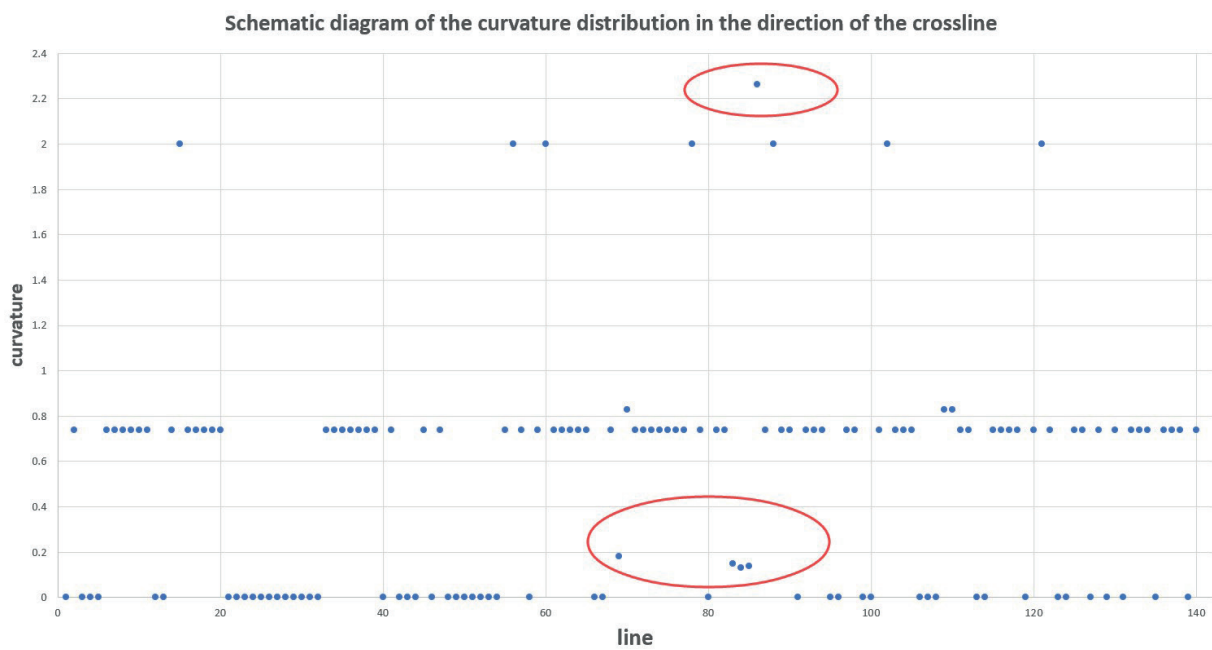


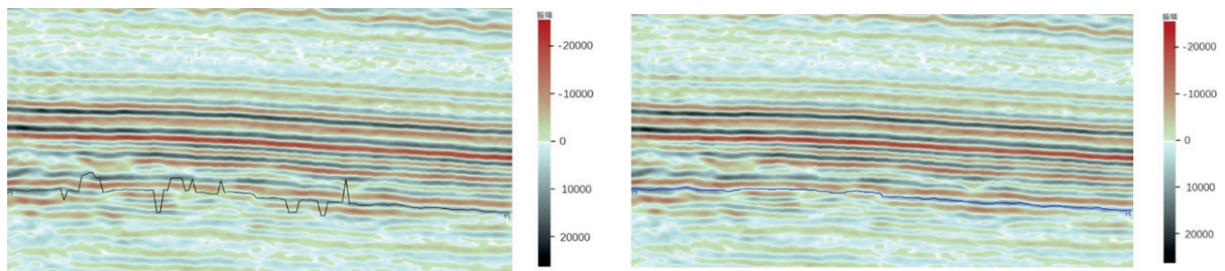
**Figure 13.** Scatter diagram of curvature distribution of a profile.



### 3. The practical application

A survey has 142 inline, 110 crossline, 401 sampling points, and the sampling interval is 1ms. We select the start track, middle track, and end track to generate the initial seed point.

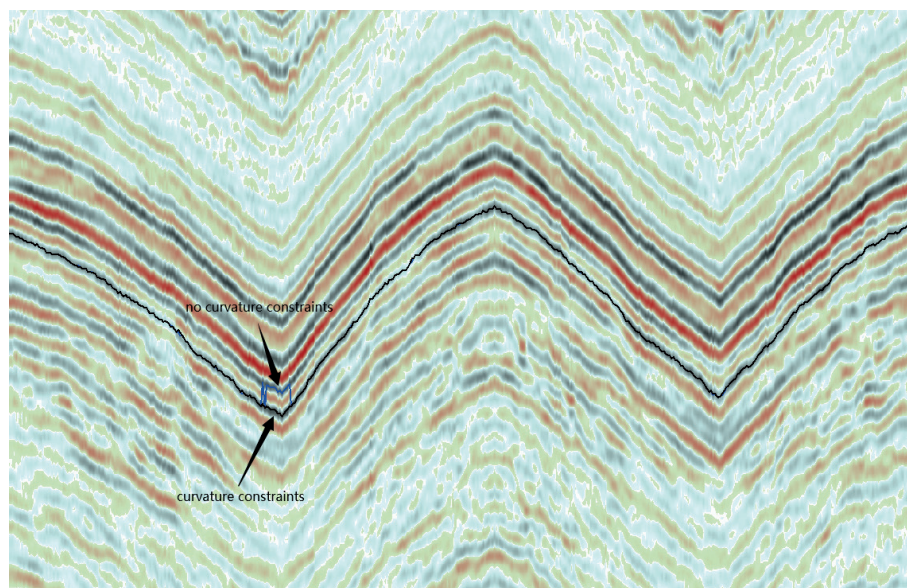
This survey is tracked, and the tracking result is shown in Figure 14. Where a is the tracking result without curvature constraint, and b is the tracking result under curvature constraint. Furthermore, Figure 15 shows the results of arbitrary line comparison between the two horizons. It can be seen from Figure 14 and 15 that curvature has a good constraint effect on tracking results.



(a) Horizon without curvature constraint

(b) Horizon under curvature constraint

**Figure 14.** Actual data test results.



— No curvature constraint horizon

— Curvature constraint horizon

**Figure 15.** Arbitrary line horizon.

Meanwhile, this paper also compares the current popular deep learning-based horizon tracking results with the tracking results of this paper (Figure 16). The following table lists related parameters.

It can be seen from the Table 1. the method in this paper has higher tracking efficiency than the deep learning method, and requires fewer labels and computer memory than deep learning. From the comparison of the base maps in Figure 17 and Figure 18, it can be seen that the result of curvature constraint method is smoother and has better results, which can also be proved from Figure 16.



## Automatic horizon tracking algorithm with curvature constraint

Method	Time consumed	Label ratio	Memory consumption
Deep learning	3.5 h	4.83%	8 GB
Curvature constraint	60 s	2.72%	6 GB

**Table 1.** Comparison of Horizontal Tracking Methods Based on Deep Learning and Curvature Constraints.

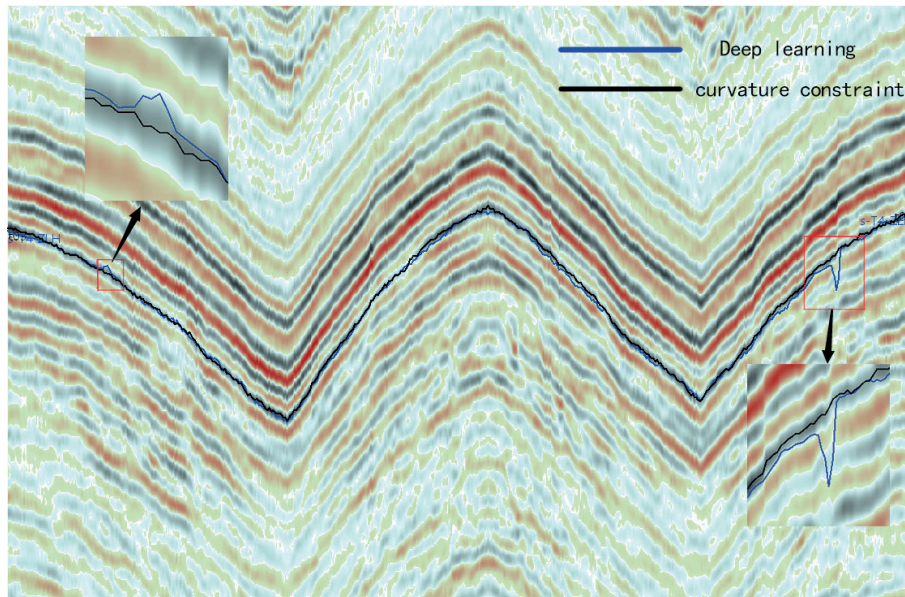


**Figure 16.** Comparison of deep learning and curvature constraint horizon.

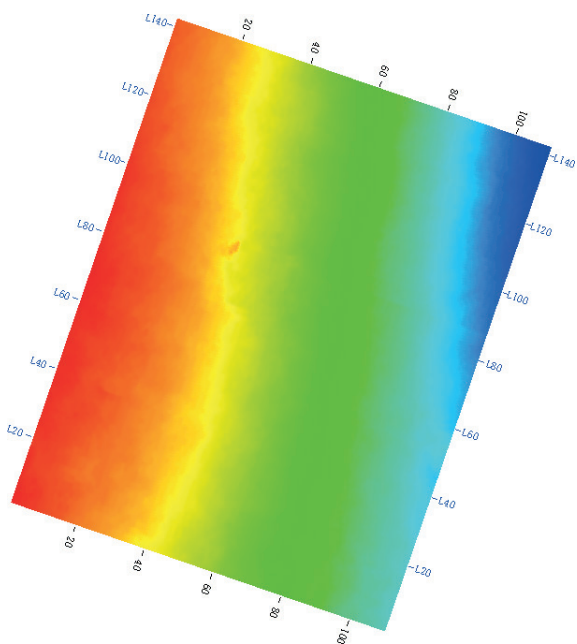


**Figure 17.** Curvature constraint horizon.

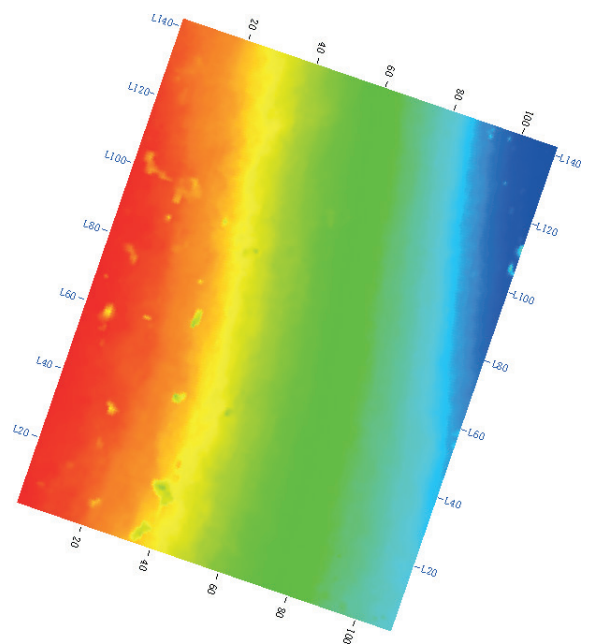


**Figure 18.** Deep learning horizon.

## 4. Conclusions

In view of the low precision and low efficiency of manual interpretation in traditional horizon interpretation. In this paper, a combination of mathematical curvature and coherence principles is proposed, and an automatic horizon tracking algorithm is proposed. High accuracy and efficiency have been achieved, and verified by actual data, the curvature has a good constraining effect on the tracking results, and has application prospects in actual production. However, when there is a fault in the area, this algorithm cannot cross the fault automatic well, and the tracking algorithm across the fault automatic is also one of the next research directions.

**Acknowledgment.** This work is supported by Science & Technology Research and Development Project of CNPC (2021DJ3505) and the Open Foundation of the Key Laboratory of Geophysics Project of CNPC “Grant No: 2022-KFKT-25”.

## References

- Alberts P., K. Moorfeld K. (1999). Artificial neural networks for simultaneous multi horizon discontinuities[C]. Expanded Abstracts of 61st EAGE Annual Conference, 6031-6034.
- Luo, C. (2014). Research on the method of target feature recognition in 3D seismic images[D], University of Electronic Science and Technology of China.
- Department of Mathematics, Tongji University. (1996). Advanced mathematics., Higher Education Press, 209-210.
- Labrunye E., C. Carn (2015). Merging chronostratigraphic modeling and global horizon tracking. Interpretation, 3, 2, 59-67.
- Forte E., M. Dossi, M. Pipan. A. Del Ben (2016). Automated phase attributebased picking applied to reflection seismic, Geophysics, 8, 2, 1942-2156.
- Hakami A, M., K, J Marfur and S. Al-Dossary (2004). Curvature Attribute and seismic interpretation: Case study from Fort Worth Basin, Texas, USA. SEG Technical Program Expanded Abstracts 74th Annual Meeting. Denver, Colorado, 2586.
- Hongxing Li, Cai Liu, Chunhui Tao. (2007). Application of Image Edge Detection Method in Automatic Detection of Seismic Section Events[J]. Advances in Geophysics, 22, 5, 4.
- Liuxin Y., S. Z. Sun (2020). Seismic horizon tracking using a deep convolutional neural network, J. Petroleum Sci. Engin., 187, 106709.
- Ming Cheng, Junxing Cao, Jiachun You, Jun Wang, Jun Liu. (2021). Automatic horizon tracking method based on image semantic segmentation [J]. Adv. Geophys., 36, 04, 1504-1511.
- Peters B, J. Granek, E. Haber (2019). Multiresolution neural networks for tracking seismic horizons from few training images[J]. Interpretation, 7, 3, SE201-SE213.
- Roberts A. (2001). Curvature attributes and their application to 3D interpreted horizon, First Break, 19, 2, 85-100.
- Xuyue Liu, Wei Zhou, Bing Zhang, Jun Huang. (2017). An automatic tracking method for seismic horizons based on imagery[J]. Geophysical and Geochemical Exploration Computing Technology, 39, 01, 64-70.
- Xuesen Li (2005). Research on three-dimensional visualization display technology of seismic reflection horizon structure information[J]. Adv. Geophys., 20, 3, 735-740.
- Yinghao Yuan (2020). Research on the Interpretation Method of Seismic Reservoir Image Based on Deep Learning [D]. University of Electronic Science and Technology of China.
- Yue Yu, Shangxu Wang, Sanyi Yuan, Wenjing Sang, Shuai Chen. (2021). Seismic horizon automatic picking method based on improved U-Net [C]. Proceedings of the Fourth Annual Conference on Oil and Gas Geophysics. 602-605.

\*CORRESPONDING AUTHOR: Huiqun XU,

School of Geophysics and petroleum resources, Yangtze University, Wuhan 430100, Hubei Province  
e-mail: huiqunxu@yangtzeu.edu.cn